

Research Article

Cite this article: Khammanee T *et al.* (2025) Characterization and microRNA quantification of plasma-derived extracellular vesicles in patients with *Plasmodium knowlesi* infection. *Parasitology* **152**, 381–394. <https://doi.org/10.1017/S0031182025000423>

Received: 8 May 2024

Revised: 10 February 2025

Accepted: 6 March 2025

First published online: 26 March 2025

Keywords:














bioinformatic analysis; extracellular vesicle; microRNA; *P. knowlesi*; RT-qPCR

Corresponding author:

Supinya Thanapongpichat;

Email: supinya.th@psu.ac.th

Characterization and microRNA quantification of plasma-derived extracellular vesicles in patients with *Plasmodium knowlesi* infection

Thunchanok Khammanee¹ , Natakorn Nokchan² , Piyatida Molika² , Hansuk Buncherd³ , Kanitta Srinoun³ , Natta Tansila³ , Charinrat Saechan³ , Rachanida Paparatana³ , Nongyao Sawangjaroen¹ , Suwannee Jitueakul⁴, Chatree Ratcha⁵, Churat Weeraphan⁶ , Jisnusun Svasti⁶ , Raphatphorn Navakanitworakul²  and Supinya Thanapongpichat³ 

¹Division of Biological Science, Faculty of Science, Prince of Songkla university, Songkhla Thailand; ²Department of Biomedical Sciences and Biomedical Engineering, Faculty of Medicine, Prince of Songkla University, Songkhla, Thailand; ³Faculty of Medical Technology, Prince of Songkla University, Songkhla, Thailand; ⁴Haematology Unit, Department of Medical Technology and Pathology, Suratthani Hospital, Surat Thani, Thailand; ⁵Medical Technology Laboratory, Phanom Hospital, Surat Thani, Thailand and ⁶Laboratory of Biochemistry, Chulabhorn Research Institute, Bangkok, Thailand

Abstract

MicroRNAs (miRNAs), derived from extracellular vesicles (EVs) are circulating intercellular communicators which influence pathogenesis and could be used as potential diagnostic markers. In this study, plasma-derived EVs from *Plasmodium knowlesi*-infected patients ($n = 13$) and healthy individuals ($n = 10$) were isolated using size exclusion chromatography and ultracentrifugation. The presence of EVs was confirmed by transmission electron microscopy and Western immunoblotting, and quantified by nanoparticle tracking analysis. The EVs isolated from patients exhibited a larger size, accompanied by an elevated concentration of EVs. The relative expression levels of 8 human miRNAs were quantified using reverse transcriptase quantitative polymerase chain reaction. Compared to uninfected groups, hsa-miR-223-5p (P -value = 0.0002) and hsa-miR-486-5p (P -value = 0.025) were upregulated in *P. knowlesi*-infected patients. Bioinformatic analysis revealed that these miRNAs are predicted to target both human host and parasite genes, and they were found to be enriched in various malaria-related pathways. The areas under the receiver operating characteristic curve of hsa-miR-223-5p and hsa-miR-486-5p were 0.9154 and 0.8231, respectively, suggesting the potential of EV-miRNAs as diagnostic markers. Results revealed that EV-miRNAs may play a significant role in the progression of *P. knowlesi* infection. Further investigations should explore their potential impact on gene expression regulation as diagnostic biomarkers or targets for therapeutic interventions.

Introduction

Extracellular vesicles (EVs) are small lipid-bound vesicles that cells release either directly from the plasma membrane or through endosomal mechanisms, which merge with the membrane before entering the extracellular space (Théry *et al.*, 2018). In the context of malaria infection, increased EV levels in the bloodstream have been observed to correlate with disease severity and clinical symptoms. These EVs, sourced from a variety of cells including infected erythrocytes, platelets, leucocytes and endothelial cells, are typically major contributors to malaria-derived EVs, with infected erythrocytes being a significant source (Combes *et al.*, 2004; Pankoui Mfonkeu *et al.*, 2010; Sahu *et al.*, 2013; Abels and Breakefield, 2016). Platelets and reticulocytes play prominent roles in *Plasmodium vivax* infections as the main contributors to EV production (Toda *et al.*, 2020). EVs play a significant role in the biological and pathogenic processes of malaria. EVs, originating from both host and parasite cells, transfer cell-specific biomolecules to immune cells or parasitized cells, influencing the inhibition or promotion of cytokine secretion, thereby inducing inflammation, promoting parasite survival or facilitating gametocyte formation (Mantel *et al.*, 2013; Regev-Rudzki *et al.*, 2013; Sisquella *et al.*, 2017).

MicroRNAs (miRNAs) are small non-coding RNA molecules that are secreted from cells into the bloodstream where they can either be bound to proteins or packaged into EVs. miRNAs participate in post-transcriptional gene regulation predominantly by binding to the 3' untranslated region (3'UTR) of the target messenger RNA (mRNA), but they can also bind

© The Author(s), 2025. Published by Cambridge University Press. This is an Open Access article, distributed under the terms of the Creative Commons Attribution-NonCommercial licence (<http://creativecommons.org/licenses/by-nc/4.0/>), which permits non-commercial re-use, distribution, and reproduction in any medium, provided the original article is properly cited. The written permission of Cambridge University Press must be obtained prior to any commercial use.

to the 5'UTR or even within the coding region of the mRNA, leading to protein translation inhibition or mRNA degradation (Schuster and Hsieh, 2019). *P. falciparum* is unable to produce miRNAs and lacks genes encoding Argonaute and Dicer (Xue et al., 2008). In this context, human miRNAs are involved in modulating gene expression in both *Plasmodium* parasites and human hosts, affecting the host immune response, inflammation, tissue damage, survival and replication of the parasite throughout the life cycle (Lodde et al., 2022). In mild to severe malaria, the dysregulation of gene expression involved in immune regulation is marked by miRNAs such as miRNA-16, miRNA-155, miRNA-150, miRNA-223 and miRNA-451, indicating the potential of these miRNAs as biological markers for malaria infection (Rangel et al., 2019). Children with severe malaria showed increased expression of plasma miR-3158-3p, linked to seizures, and hsa-miR-4497, which is associated with parasite biomass and HRP2 levels. Both miRNAs are associated with acute respiratory distress syndrome (Gupta et al., 2021). In the serum of *P. vivax*-infected patients, levels of miR-451 and miR-16 are decreased, while the level of miR-223 is not changed (Chamnanchanunt et al., 2015). The reduction was likely due to red blood cell degradation and miRNA clearance by the spleen. In *P. vivax* patients, other studies have demonstrated notably elevated plasma levels of miR-191, miR-223, miR-145 and miR-155 (Hadighi et al., 2022). An increase in miR-4454 and miR-7975 was also observed in patients with severe thrombocytopenia (Santos et al., 2021). Human miRNA has been found to be transferred to the intracellular parasite and regulate gene expression, with involvement in pathogenicity and host defence mechanisms (LaMonte et al., 2012; Dandewad et al., 2019). The overexpression of miR-451, miR-223 and let-7i in *P. falciparum* within sickle cell erythrocytes can regulate parasite genes, leading to a reduction in growth (LaMonte et al., 2012). *Plasmodium apicortin* targeted by miR-150-3p and miR-197-5p also impaired the growth and invasion of the malaria parasite (Chakrabarti et al., 2020). miRNAs found in both plasma and EVs are important diagnostic markers due to their stability in the bloodstream (Mantel et al., 2016). Notably, EV-derived miRNAs directly reflect the pathological characteristics of their cellular origin (Xu et al., 2022). EVs derived from *P. falciparum* cultures with infected red blood cells (iRBCs) showed high expression levels of specific small RNAs, while miR-451a, miR-486-5p, miR-92a-3p, miR-103a-3p, let-7b-5p, miR-181a and miR-106b-5p were particularly prominent in the small RNA profile of these EVs (Mantel et al., 2016; Wang et al., 2017; Babatunde et al., 2018). *P. falciparum* EVs carrying miRNA-451 downregulate target genes (*CAV-1* and *ATF-2*) in endothelial cells, affecting vascular function (Mantel et al., 2016). Wang et al. demonstrated host-miRNA regulation, specifically showing that miR-451 and miR-140 from large EVs downregulate *VAR* genes encoding *P. falciparum* erythrocyte membrane protein (*PfEMP1*) (Wang et al., 2017). The expression of miRNA varies in different physiological conditions associated with the development of pathological diseases and organ damage. However, the expression of EV-derived miRNA from patient plasma in *Plasmodium knowlesi* malaria is not well studied.

P. knowlesi primarily resides in monkeys but can infect humans as a zoonotic disease transmitted through mosquito vectors. Infections caused by *P. knowlesi* range from asymptomatic cases to severe malaria, presenting with anaemia, acute respiratory distress, renal failure and thrombocytopenia, and can potentially be fatal. Its 24-h intraerythrocytic cycle accelerates parasitaemia and disease progression (Anstey et al., 2021), leading to severe outcomes or death if not promptly diagnosed and treated (Cox-Singh et al., 2010; Rajahram et al., 2012; Chantaramongkol and

Table 1. Characteristics of the study subjects

Characteristic	<i>P. knowlesi</i> patient (n = 13)	Healthy donor (n = 10)	P-value
Sex, male (%)	53.85	40	0.6802 ^a
Age, years (mean ± s.d.)	41.8 ± 13.122	36 ± 5.963	0.1107 ^b

^aFisher's exact test.

^bMann-Whitney U test.

Buathong, 2016). In Thailand, *P. knowlesi* cases, once rare, have been steadily increasing. According to the Thai National Malaria Control Program, reported cases rose from 6 out of 11 595 in 2017 to 259 out of 16 680 in 2023 (ThaiMOPH, 2024).

The identification of EVs and miRNAs can help elucidate the molecular processes that contribute to these complications, potentially leading to better diagnostic tools and targeted interventions.

Materials and methods

Blood sample collection and processing

Peripheral blood samples were obtained from individuals infected with the *P. knowlesi* parasite and from healthy donors. The blood specimens were obtained using leftover EDTA-containing tubes from the hospital in Southern Thailand. This study was approved by the Ethical Committee of the Faculty of Medical Technology, Prince of Songkla University (EC66-03). The characteristics of 13 *P. knowlesi* patients and 10 healthy donors are shown in Table 1. All *P. knowlesi* patients were confirmed by nested polymerase chain reaction (PCR) (Putaporntip et al., 2011). The blood samples were centrifuged at 1500 g for 10 min. The resulting plasma was then subjected to another round of centrifugation at 2500 g for 15 min at 4°C, twice, to obtain platelet-free plasma. A 0.5–1-mL aliquot of the plasma supernatant was preserved at –80°C until further isolation of EVs.

EVs enrichment using size exclusion chromatography and ultracentrifugation

A commercial size exclusion chromatography (SEC) qEV1/35 nm column from iZON Sciences (Christchurch, New Zealand) was used to isolate EVs from the plasma samples following the manufacturer's instructions (Fig 1A). The column was equipped with an automatic fraction collector. Before sample separation, the column was pre-equilibrated with phosphate-buffered saline (PBS), which was previously filtered in a sterile manner through a 0.22-µm filter. For each isolation, 700 µL of plasma was loaded onto the top of the qEV column. Subsequently, 4 fractions (700 µL per fraction) were immediately collected into separate 1.5-mL microcentrifuge tubes. To further concentrate the EVs, the pooled fractions were subjected to ultracentrifugation (UC) at 120 000 g for 90 min. After centrifugation, the EV pellet was resuspended in PBS, resulting in a final volume of 100 µL.

Transmission electron microscopy

The EVs were subjected to a fixing process using a 2.5% glutaraldehyde solution. Subsequently, these fixed EVs were carefully placed onto a Formvar carbon grid. To enhance visualization, the grids were treated with a 2% uranyl acetate stain and then allowed to dry at ambient temperature. Finally, the dried grids were observed and

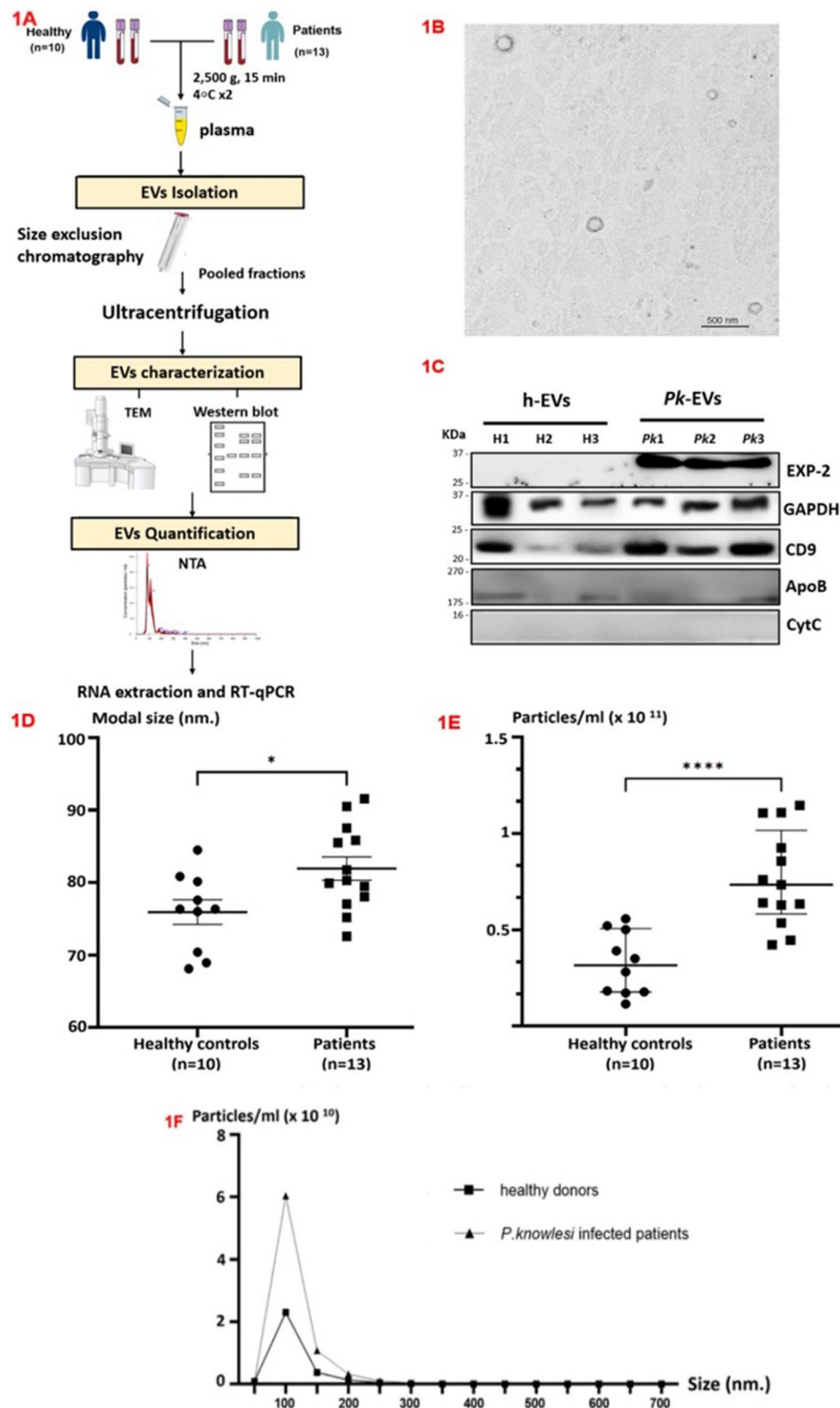


Figure 1. Isolation and characterization of plasma EVs. (A) Schematic overview of experimental methods. (B) Transmission electron microscopy. (C) Western blot detection of EXP-2, GAPDH, CD9, ApoB and Cytochrome C1 (CYC1). (D) Mode size and (E) concentration between patients and uninfected individuals, compared using the unpaired 2-tailed *t*-test. Data are presented as mean values with SEM. (F) Size distribution of extracellular particles (nm) versus concentration (particles/mL) (**P* < 0.05, *****P* < 0.0001).

analysed using an advanced Talos™ F200i transmission electron microscope manufactured by Thermo Scientific (MA, USA).

Western blot analysis

For immunoblotting analysis, 10 µg of isolated EVs were mixed with 5× loading buffer and then heated at 100°C for 5 min. Subsequently, the EV proteins were separated on a 12% polyacrylamide gel. Proteins were then transferred to polyvinylidene fluoride (PVDF) membranes. The membranes were blocked using 5% non-fat milk in tris-buffered saline (TBS) for 1 h. After blocking, the membrane was washed thrice with TBS-T (TBS with 0.1% Tween 20) for 10 min. The primary antibodies, including anti-rabbit CD9 (Abcam ab223056) (Abcam, Cambridge, UK) at a dilution of 1:2000 and anti-mouse GAPDH (Abcam ab8245) at a dilution of 1:20 000, were diluted in 1% non-fat milk in TBS-T and used as positive markers for EVs. The anti-cytochrome C1 (BioLegend, CA, USA) and anti-rabbit APOB (Abcam ab139401) were diluted at 1:1000 as non-EV markers and indicators of lipoprotein contamination, respectively. The anti-mouse EXP-2 (The European Malaria Reagent Repository, Cat# 7.7) was diluted at 1:600 to detect against the parasitophorous vacuole membrane (PVM). After incubating with the primary antibodies, the PVDF membrane was washed thrice with TBS-T buffer for 10 min. For secondary detection, secondary antibodies were applied at a dilution of 1:5000 and incubated at room temperature for 1 h. An ultra-sensitive enhanced chemiluminescent (ECL) horseradish peroxidase substrate was employed to visualize the specific proteins.

Quantification of EVs

Nanoparticle tracking analysis (NTA) was employed to determine the size and concentration of the EVs. The NTAs were carried out using a NanoSight NS300 NTA 3.4 system equipped with a 488-nm laser. To conduct the analyses, aliquots of the isolated EVs were diluted 500–1000-fold with 0.22-µm filtered deionized water, ensuring that the number of particles per frame fell within the range of 20–100. The camera level for each sample was set at 13, and the detection threshold was set at 5. The NTA software analysed 5 videos for 60 s each in duplicate, while the temperature of the laser unit was maintained at 25°C. The obtained NTA data were compared for size distribution, modal size, and concentration of particles between the *P. knowlesi* infection and healthy donor groups.

RNA extraction and reverse transcriptase quantitative PCR

The instructions provided by the manufacturer of an RNA extraction kit were followed to isolate total RNA. Initially, 350 µL of lysis buffer was added to the EV sample. The mixture was briefly vortexed and incubated for 5 min at room temperature. Next, 100% ethanol was added to the sample, and the resulting mixture was transferred to a spin column and centrifuged at 13 000 rpm for 1 min. After washing, the isolated RNA was eluted from the spin column using 50 µL of elution buffer. The quantification of RNA was performed using a NanoDrop spectrophotometer. The complementary DNA (cDNA) was generated using a QuantiMir reverse transcription kit from System Biosciences. Subsequently, amplification was performed with specific miRNA primers, as detailed in Table 2. The amplification was carried out in a total volume of 20 µL PCR mixture which contained 10 µL of 2X qPCR-BIO SyGreen Mix, 0.4 µM of each primer, and 1 µL of cDNA. The

amplification thermal condition consisted of 95°C for 1 min followed by 40 cycles of 95°C for 15 s and 60°C for 1 min. Each sample was analysed in triplicate, with the negative control as nuclease-free water. Technical replicates with a standard deviation exceeding 0.5 were excluded and retested.

miRNA expression analysis

Quantification cycle (Cq) values were used to compare the relative quantities of miRNAs between the malarial and healthy samples. The Delta Cq (ΔCq) of the target miRNA was calculated by averaging triplicate values and subtracting them from the average Cq values of miR-451a in the corresponding samples. The hsa-miR451a-5p was used as a normalization control. $\Delta\Delta Cq$ was then normalized by comparing the ΔCq of each sample to the mean ΔCq of the healthy control group. The expression of EV miRNA was assessed using the comparative Cq method ($-2^{\Delta\Delta Cq}$).

Target gene prediction and enrichment analysis

The target genes of upregulated miRNAs were predicted using TargetScan Release 8.0 (https://www.targetscan.org/vert_80/), miRDB (<https://mirdb.org/>), miRDIP (<https://ophid.utoronto.ca/mirDIP/>), and miRTarBase (<https://mirtarbase.cuhk.edu.cn/>). The human genes related to malaria infection were retrieved from the Kyoto Encyclopedia of Genes and Genomes (KEGG) malaria pathway. The candidate targets that overlapped between the miRNA target database and the malaria pathway in the KEGG database were selected using a Venn diagram. The Gene Ontology (GO) and KEGG enrichment analyses of individual miRNAs were conducted using the DIANA-miRPath v.4.0 (<https://diana-lab.e-ce.uth.gr/app/miRPathv4>) and DAVID gene annotation tool (<https://david.ncicrf.gov/>). The prediction in DIANA-miRPath was based on experimentally supported targets from TarBase 8.0. The pathway union option was used, with false discovery rate (FDR) correction. The bar and bubble plots were generated using SRplot (<https://www.bioinformatics.com.cn/srplot>). The *P*-values were calculated by Fisher's exact test and the FDR was obtained by the Benjamini–Hochberg method. FDR values less than 0.05 were considered statistically significant for enrichment analysis. The DAVID online tool was conducted for upregulated miRNA, and *P*-value < 0.05 was set as a significant threshold.

The transcriptome data of *P. knowlesi* were retrieved from the PlasmoDB 8.0 database to determine the target binding of human miRNAs with *P. knowlesi* transcripts. Subsequently, an analysis of the selected miRNA sequences was conducted against the *P. knowlesi* strain H transcriptome using the psRNATarget tool (<http://plantgrn.noble.org/psRNATarget/>) with default recommended value of 5 (Dai *et al.*, 2018).

Statistical analysis

All data were presented as the mean and standard error of the mean (SEM), with normality assessed using the D'Agostino–Pearson test. Student's *t*-test was used to assess differences in mode size and concentration of EVs between groups. The non-parametric Mann–Whitney *U* test was used to compare the expression levels of miRNAs between the plasma-derived EVs of healthy individuals and patients. This statistical analysis was conducted using GraphPad Prism software (version 9.0; GraphPad Software, San Diego, CA, USA). Receiver operating characteristic (ROC) curve analysis was performed to evaluate the diagnostic potential of

Table 2. MiRNA sequences and Cq values

miRNA	miRbase accession number	Sequence (5'-3')	Mean Cq \pm SEM			
			Uninfected		<i>P. knowlesi</i> infection	
hsa-miR-451a	MIMAT0001631	AAACCGUUACCAUUCAGAGUU	27.22	± 0.55	28.08	± 0.25
hsa-miR-150-5p	MIMAT0000451	UCUCCCAACCCUUGUACCAGUG	27.53	± 0.55	28.52	± 0.44
hsa-miR-486-5p	MIMAT0002177	UCCUGUACUGAGCUGCCCCGAG	27.09	± 0.82	26.80	± 0.32
hsa-miR-15b-5p	MIMAT0000417	UAGCAGCACAUCAUGGUUUACA	28.82	± 0.46	30.61	± 0.47
hsa-miR-16-5p	MIMAT0000069	UAGCAGCACGUAAAUAUUGGCG	27.79	± 0.73	29.98	± 0.65
hsa-let-7a-5p	MIMAT0000062	UGAGGUAGUAGGUUGUAUAGUU	28.8	± 0.43	30.23	± 0.46
hsa-miR-223-5p	MIMAT0004570	CGUGUAUUUGACAAGCUGAGUU	29.48	± 0.48	28.52	± 0.31
hsa-let-7b-5p	MIMAT0000063	UGAGGUAGUAGGUUGUGUGUU	30.31	± 0.15	30.9	± 0.25
hsa-miR-106b-5p	MIMAT0000680	UAAAGUGCUGACAGUGCAGAU	30.83	± 0.25	32.36	± 0.31

Table 3. Evaluation of miRNA expression between healthy controls and patients

miRNA	Mean $\Delta Cq \pm$ SEM				Mean relative expression ($2^{-\Delta\Delta Cq}$) \pm SEM				
	Uninfected		<i>P. knowlesi</i> infected		Uninfected		<i>P. knowlesi</i> infected		<i>P</i> -value
hsa-miR-150-5p	0.31	± 0.2	0.44	± 0.58	1.10	± 0.18	1.77	± 0.49	0.66
hsa-miR-486-5p	-0.13	± 0.31	-1.27	± 0.31	1.20	± 0.22	2.84	± 0.56	0.025
hsa-miR-15b-5p	1.6	± 0.32	2.53	± 0.5	1.27	± 0.33	0.95	± 0.28	0.343
hsa-miR-16-5p	0.57	± 0.28	1.9	± 0.7	1.16	± 0.18	1.42	± 0.67	0.166
hsa-let-7a-5p	1.58	± 0.39	2.15	± 0.59	1.33	± 0.31	1.24	± 0.3	0.648
hsa-miR-223-5p	2.05	± 0.44	0.44	± 0.15	1.29	± 0.24	3.27	± 0.26	0.0002
hsa-let-7b-5p	3.09	± 0.66	2.82	± 0.41	1.95	± 0.58	2.03	± 0.7	0.927
hsa-miR-106b-5p	3.61	± 0.5	4.28	± 0.35	1.66	± 0.54	0.89	± 0.22	0.313

miRNA expression levels for *P. knowlesi* infection. ROC curve analysis was carried out using delta Ct values (Canatan et al., 2022). The accuracy of the test was assessed by measuring the area under the ROC curve (AUC), which identified optimal sensitivity and specificity levels for distinguishing normal individuals from patients.

Results

Characterization of plasma-derived EVs

Transmission electron microscopy (TEM) and Western blot analysis were used for EV characterization to evaluate the presence of the EVs isolated through SEC- and UC-based methods (Fig 1A). TEM revealed spherical phospholipid bilayer structures with an diameter of approximately 100 nm (Fig 1B). As shown in Fig 1C, EVs demonstrated enrichment of exosomal protein markers including CD9 and glyceraldehyde-3-phosphate dehydrogenase (GAPDH), while Cytochrome C1 (CYC1) (non-EV marker) was not detected. The presence of parasite proteins EXP-2 was determined in EVs from *P. knowlesi* malaria patients. A signal for ApoB lipoprotein found in chylomicrons very-low-density lipoprotein, intermediate-density lipoprotein and low-density lipoprotein (LDL) particles was observed.

Quantification of EVs' size and concentration

The size and concentration distribution for each biological replicate were determined through NanoSight analysis. The particles

displayed diameters ranging from under 50 to 600 nm, with most falling within the 50–100 nm size category. The 250–600 nm size range accounted for less than 1% of the total, indicating the presence of aggregated vesicles. The average modal size of isolated EVs from *P. knowlesi*-infected individuals (*Pk*-EVs) was 81.9 ± 1.75 nm, which was significantly larger than those from healthy donors (*h*-EVs) at 75.9 ± 1.25 nm (*P*-value = 0.019) (Fig 1D). The size was consistent with the results of TEM. Larger EVs observed by the nanoparticle tracking system were possibly the result of aggregate formation. A statistically significant 2.4-fold increase in particle concentration was recorded for *P. knowlesi*-infected patients, measuring 7.64×10^{10} particles/mL (range: 4.21×10^{10} – 1.15×10^{11} particles/mL) compared to healthy donors, with concentration 3.24×10^{10} particles/mL (range: 1.15×10^{10} – 5.56×10^{10} particles/mL), *P*-value < 0.0001 (Fig 1E). The size versus concentration of the 2 groups is illustrated in Fig 1F. The mean concentration of extracellular particles within the 1–50 nm size range was higher in healthy donors compared to those with *P. knowlesi* infection (8.32×10^8 vs. 7.2×10^8). In the peak graph showing the 50–100 nm size range, the *P. knowlesi* infection group exhibited a significantly higher concentration at 6.03×10^{10} particles/mL, in contrast to 2.35×10^{10} particles/mL in healthy donors.

Relative expression of miRNAs

The SYBR Green quantitative PCR (qPCR)-based detection methods were used to evaluate the expression of 8 specific human miRNAs. The average Cq, ΔCq and $2^{-\Delta\Delta Cq}$ values for all miRNAs were calculated (Tables 2 and 3), with hsa-miR-451a-5p serving

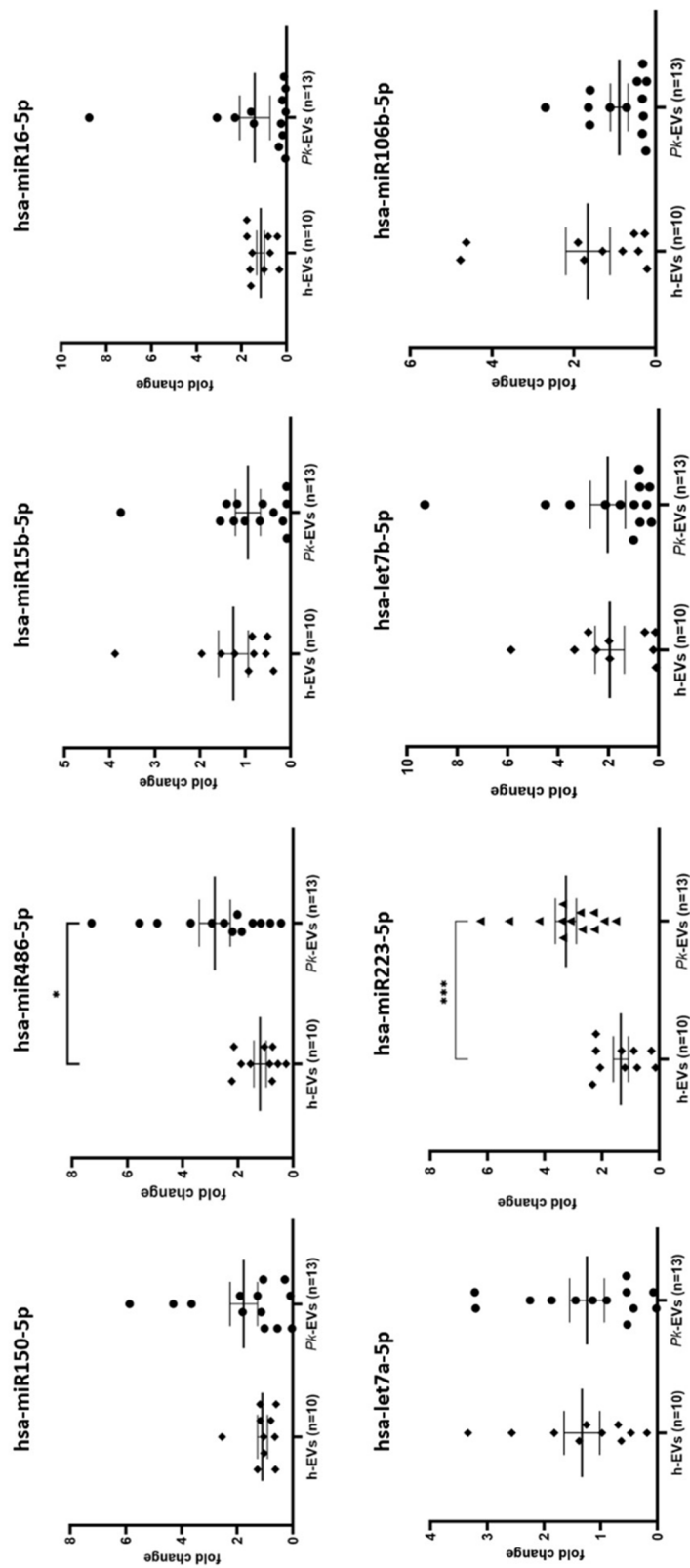


Figure 2. Dot plots of miRNA relative expression in EVs derived from healthy controls and *P. knowlesi*-infected individuals. Graphs display mean levels with SEM. Differences between the 2 groups were assessed by using the non-parametric Mann–Whitney *U* test (**P* < 0.05, ****P* < 0.001).

Table 4. Potential human target genes of hsa-miR-223-5p- and hsa-miR-486-5p-related malaria pathway

miRNA	Target transcript	Target prediction database
hsa-mir-223-5p	HGF	TargetScan, miRDB
	MET	TargetScan, miRDIP
	TLR4	TargetScan
	MYD88	TargetScan
	GYPA	TargetScan
	GYPC	TargetScan
	VCAM1	TargetScan
hsa-mir-486-5p	CD40	TargetScan
	CD40	miRDIP, mirTarBase

GYPC: glycyphorin C, HGF: hepatocyte growth factor, CD40: cluster of differentiation 40, TLR4: toll-like receptor 4, GYPA: glycyphorin A, MYD88: myeloid differentiation primary response protein 88, MET: MET Proto-Oncogene, Receptor Tyrosine Kinase, VCAM1: vascular cell adhesion molecule 1.

as the endogenous control for data normalization. The relative expression of EV-miRNAs in malaria compared to healthy donors is shown in Fig 2. The reverse transcriptase qPCR (RT-qPCR) results revealed a significant increase in levels of hsa-miR-223-5p (P -value = 0.0002) and hsa-miR-486-5p (P -value = 0.008) in *Pk*-EVs group. The other 6 miRNAs showed no significant differences in expression levels between *P. knowlesi* infection and healthy individual groups.

miRNA target prediction, GO and KEGG enrichment analysis

Prediction of the human-host gene targets for hsa-miRNA-223-5p and hsa-miRNA-486-5p utilized information from 4 databases. Results showed that 8 and 1 computationally predicted targets were identified for hsa-miR-223-5p and hsa-miR-486-5p, respectively (Table 4). Intriguingly, *CD40* was a shared target gene for both miRNAs. A pathway analysis of individual miRNAs was conducted using DIANA miRPath. Notably, no enriched pathways associated with hsa-miRNA-223-5p were observed in this analysis. By contrast, hsa-miRNA-486-5p showed enrichment in GO terms related to protein binding for molecular function; cytosol, cytoplasm and ribonucleoprotein complex for cellular component (CC) (Fig 3A), demonstrating significant enrichment in the KEGG pathways of the EGFR (epidermal growth factor receptor) tyrosine kinase inhibitor resistance pathway. DAVID was employed to determine overrepresented GO terms and KEGG pathways associated with hsa-miRNA-223-5p. This tool conducted functional and pathway enrichment analysis based on the predicted target genes of hsa-miRNA-223-5p. The top 10 ranked GO terms and KEGG pathways are displayed in Fig 3B and 3C, respectively. For GO BP, the predicted target genes were significantly enriched in phagocytosis, cellular response to mechanism stimulus, and positive regulation of NF- κ B transcription factor activity, while for GO CC, the enriched GO terms were cell surface, an integral component of plasma membrane and plasma membrane. In the KEGG pathway analysis, several predicted target genes were enriched in malaria, African trypanosomiasis and NF- κ B signaling pathway.

To explore potential interactions between miRNAs and *P. knowlesi* mRNAs and identify the potential gene targets of miRNAs in *P. knowlesi* mRNAs, the computational prediction software for miRNA-mRNA interactions, psRNATarget, was used. A total

of 35 and 15 target candidates, with expectation values higher than 4.5, were identified as targets for hsa-miRNA-223-5p and hsa-miRNA-486-5p, respectively, as presented in Tables 5 and 6. Both miRNAs were shown to downregulate various genes in *P. knowlesi* by cleaving mRNA or translation inhibition.

Potential of EVs-derived miRNAs as diagnostic markers

The AUC analysis was performed to investigate the possibility of miRNA-223-5p and miRNA-486-5p as potential diagnostic biomarkers. ROC curve illustrates the plot between true-positive rate (sensitivity) and false-positive rate (100-specificity). The optimal cut-off was identified as the maximum likelihood ratio, computed as sensitivity divided by (100 – specificity). The AUC was used to distinguish between the disease and healthy groups, where a value of 1 represents optimal discrimination. As shown in Fig 4, the AUC for miRNA-223-5p was 0.9154 (P -value = 0.0008). At the relative expression level of miRNA-223-5p at the optimal cut-off value of 7.692, the sensitivity was 76.92% (95% CI: 49.74–91.82%), and the specificity was 90% (95% CI: 59.58–99.49%). For hsa-miRNA-486-5p, the AUC was determined to be 0.8231 (P -value = 0.0092), with sensitivity and specificity 61.5% and 100%, respectively, when the optimal cut-off value was 6.923.

Discussion

The investigation of exosomal miRNAs in samples from malaria patients is an expanding area of research that holds the potential to improve our understanding of malarial pathophysiology. The identification of miRNAs involved in the biology and pathology of *P. knowlesi* malaria has not been extensively studied. This study characterized plasma-derived EVs and presented quantitative data on miRNAs derived from EVs. Significant differences in plasma-derived EVs were noted between malaria patients and healthy individuals, with those from patients being both larger in size and more abundant. This increase in size may be associated with pathological changes in host cells due to cellular stress, such as membrane blebbing, alterations in cell morphology and the formation of apoptotic bodies. These pathological changes can lead to the biogenesis and release of EVs of varying sizes, including larger subpopulations (Avalos-Padilla et al., 2021; Minwuyet and Abiye, 2022). Additionally, the immune response to *Plasmodium* infection may enhance EV production as part of the inflammatory response, resulting in an overall increase in both the quantity and size of EVs. The molecular mechanisms underlying the biogenesis of these different EV subpopulations may involve intracellular pathways such as endosomal sorting complexes required for transport (Opadokun and Rohrbach, 2021; Minwuyet and Abiye, 2022). The increased levels of plasma EVs observed during malaria infections result from the activation of circulating cells, particularly in severe cases (Babatunde et al., 2020). However, our study had limited data regarding clinical symptoms, haematological information or parasitaemia, which hindered the understanding of their relationships with the level of EVs. In this study, the isolated EVs included those originating from *P. knowlesi* parasites expressing the EXP-2 protein, which are situated on the PVM and are crucial for transporting proteins from the vacuole to the cytoplasm of red blood cells. These EVs may be internally generated and subsequently released externally, similar to the production of exosomes.

EV-miRNA quantification was performed using RT-qPCR targeting hsa-miR451-5p, hsa-miR150-5p, hsa-miR486-5p,

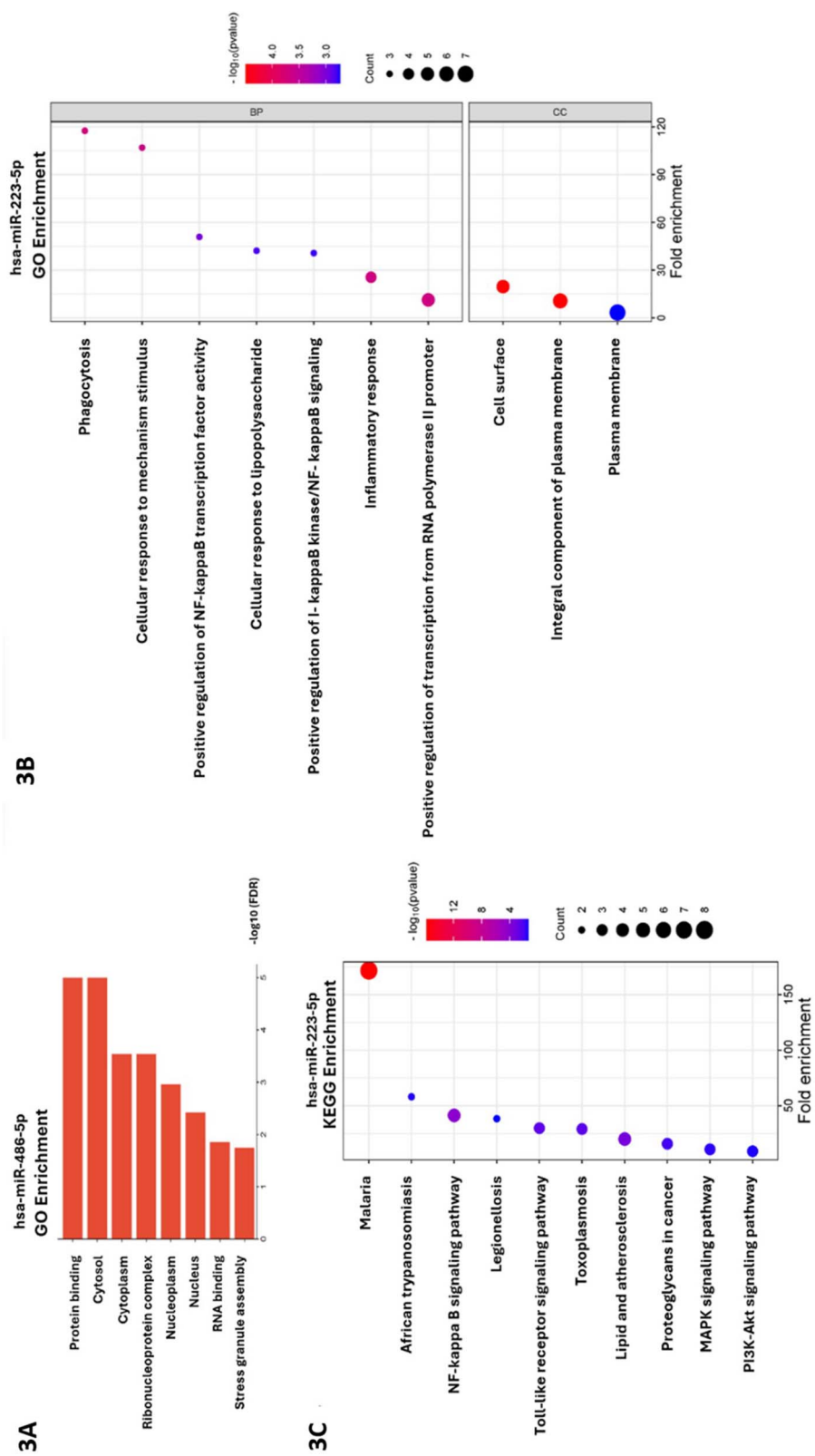


Figure 3. Gene Ontology (GO) and KEGG enrichment analysis of hsa-miR-223-5p and hsa-miR-486-5p. (A) Enriched GO terms of hsa-miR-486-5p performed using DIANA-miRPath. (B) Top 10 enriched GO terms associated with the predicted target genes of hsa-miR-223-5p and (C) top 10 enriched KEGG pathway associated with the predicted target genes of hsa-miR-223-5p. BP, biological process; CC, cellular component; DAVID, Database for Annotation, Visualization, and Integrated Discovery.

Table 5. Predicted *P. knowlesi* mRNA targets by miRNA-223-5p

Target description	miRNA start	miRNA end	Target start	Target end	Alignment	Inhibition	Expectation
<i>Plasmodium</i> protein, unknown function (PKNH_1202000)	1	22	10 449	10 470	Cleavage	4.5
DNA topoisomerase 2, putative (PKNH_0420100)	1	22	2304	2325	Cleavage	4.5
DNA replication licensing factor MCM5, putative (PKNH_1311800)	1	22	455	476	..: ..	Cleavage	4.5
Conserved <i>Plasmodium</i> protein, unknown function (PKNH_0114700)	1	22	9003	9024	Cleavage	4.5
ATP-dependent RNA helicase DHX36, putative (PKNH_1315300)	1	22	2391	2412	Cleavage	4.5
SICAvar, type I (PKNH_0940500)	1	22	2521	2542	Cleavage	4.5
Myosin B, putative (PKNH_1029900)	1	22	1494	1515	Translation	4.5
SICAvar, type I (fragment) (PKNH_0003300)	1	22	1534	1555	Cleavage	4.5
RAP protein, putative (PKNH_1120900)	1	22	2514	2535	..: ..	Cleavage	4.5
ATP-dependent DNA helicase DDX3X, putative (PKNH_0616200)	1	22	2244	2265	Cleavage	4.5
Conserved <i>Plasmodium</i> protein, unknown function (PKNH_0821400)	1	22	87	108	..: ..	Translation	4.5
Isoleucine-tRNA ligase, putative (PKNH_1444500)	1	22	1035	1055	Cleavage	4.5
DNA replication licensing factor MCM2, putative (PKNH_1340200)	1	22	2315	2336	Cleavage	5.0
Deoxyribodipyrimidine photo-lyase, putative (PKNH_1019500)	1	22	1877	1898	Cleavage	5.0
Nucleolar protein Nop52, putative (PKNH_0729800)	1	22	1714	1735	..: ..	Cleavage	5.0
Conserved <i>Plasmodium</i> protein, unknown function (PKNH_0412800)	1	22	596	618	Cleavage	5.0
D-tyrosyl-tRNA(Tyr) deacylase, putative (PKNH_0905800)	1	22	12	33	Cleavage	5.0
Conserved <i>Plasmodium</i> protein, unknown function (PKNH_1127500)	1	22	854	875	Cleavage	5.0
SICAvar, type I (PKNH_1306200)	1	22	1426	1446	Translation	5.0
GAF domain-related protein, putative (PKNH_0409800)	1	22	159	181	Cleavage	5.0
Conserved <i>Plasmodium</i> protein, unknown function (PKNH_0703500)	1	22	698	719	Translation	5.0
Dihydrouridine synthase, putative (PKNH_0716800)	1	22	1286	1307	Cleavage	5.0
Exported serine/threonine protein kinase, putative (PKNH_0313100)	1	22	4348	4369	Cleavage	5.0
Conserved <i>Plasmodium</i> protein, unknown function (PKNH_0722600)	1	22	1890	1911	Cleavage	5.0
Casein kinase 2, alpha subunit, putative (PKNH_0906000)	1	22	729	750	Cleavage	5.0
Conserved protein, unknown function (PKNH_1004400)	1	22	1374	1395	..: ..	Cleavage	5.0
Adenylyl cyclase beta, putative (PKNH_0116300)	1	22	2922	2943	Cleavage	5.0
Exoribonuclease, putative (PKNH_0707400)	1	22	2931	2952	Cleavage	5.0
Zinc finger protein, putative (PKNH_1308700)	1	22	1785	1806	..: ..	Translation	5.0
Conserved <i>Plasmodium</i> protein, unknown function (PKNH_1322200)	1	22	977	998	: ..: ..	Cleavage	5.0
Palmitoyltransferase DHHC11, putative (PKNH_0405000)	1	22	551	572	Cleavage	5.0
<i>Plasmodium</i> exported protein, unknown function (PKNH_1401200)	1	22	1959	1980	Translation	5.0
Conserved <i>Plasmodium</i> protein, unknown function (PKNH_1138300)	1	22	6674	6695	Translation	5.0
Conserved <i>Plasmodium</i> protein, unknown function (PKNH_1350500)	1	22	5901	5922	: ..: ..	Cleavage	5.0
Conserved <i>Plasmodium</i> protein, unknown function (PKNH_0506800)	1	22	3891	3912	..: ..	Cleavage	5.0

hsa-miR15b-5p, hsa-miR16-5p, hsa-miR106b-5p, hsa-miR223-5p, let7a-5p and let7b-5p. The hsa-miR451-5p was used as an endogenous control in our study due to its stable expression and relevance to the erythroid system. The miRNA-451a, which regulates erythroid differentiation and maturation, was found to be abundant in EVs under parasite culture conditions (Rathjen et al., 2006; Mantel et al., 2016; Wang et al., 2017). EVs from plasma of patients infected with *P. knowlesi* exhibited significantly higher

levels of hsa-miR-223-5p and hsa-miR-486-5p compared to those from healthy individuals, while the others showed no significant differences between the 2 groups. Exosomal miRNA expression levels changes in response to varying conditions. Different isolation techniques can capture distinct EV subpopulations based on physical properties such as size and density. Consequently, the isolated EVs may represent different subpopulations, which can influence the miRNA and biomolecule profiles observed

Table 6. Predicted *P. knowlesi* mRNA targets by miRNA-486-5p

Target description	miRNA start	miRNA end	Target start	Target end	Alignment	Inhibition	Expectation
Conserved <i>Plasmodium</i> protein, unknown function (PKNH_0946100)	1	22	5405	5426	Cleavage	4.5
Conserved <i>Plasmodium</i> protein, unknown function (PKNH_0946100)	1	22	5672	5693	Cleavage	4.5
Conserved <i>Plasmodium</i> protein, unknown function (PKNH_0718600)	1	22	894	914	Cleavage	4.5
Cyclin-dependent kinases regulatory subunit, putative (PKNH_0207700)	1	22	1870	1891	Cleavage	4.5
STAG domain-containing protein, putative (PKNH_1225300)	1	22	5318	5339	Cleavage	4.5
Conserved <i>Plasmodium</i> protein, unknown function (PKNH_0718400)	1	22	4173	4194	Cleavage	4.5
Conserved <i>Plasmodium</i> protein, unknown function (PKNH_1419000)	1	22	2861	2882	Cleavage	5.0
Conserved <i>Plasmodium</i> protein, unknown function (PKNH_1131100)	1	22	3582	3603	Cleavage	5.0
Dynein, putative (PKNH_0610000)	1	22	8085	8105	Cleavage	5.0
ATP-dependent DNA helicase DDX3X, putative (PKNH_0616200)	1	22	826	847	Cleavage	5.0
Proteasome subunit beta type-7, putative (PKNH_1200500)	1	22	532	553	Translation	5.0
Conserved <i>Plasmodium</i> protein, unknown function (PKNH_1242300)	1	22	29	50	Cleavage	5.0
Lysine-specific histone demethylase 1, putative (PKNH_1311700)	1	22	3760	3781	Cleavage	5.0
Lysine-specific histone demethylase 1, putative (PKNH_0310700)	1	22	2758	2779	Translation	5.0
S-adenosylmethionine synthetase, putative (PKNH_0720200)	1	22	991	1011	Translation	5.0

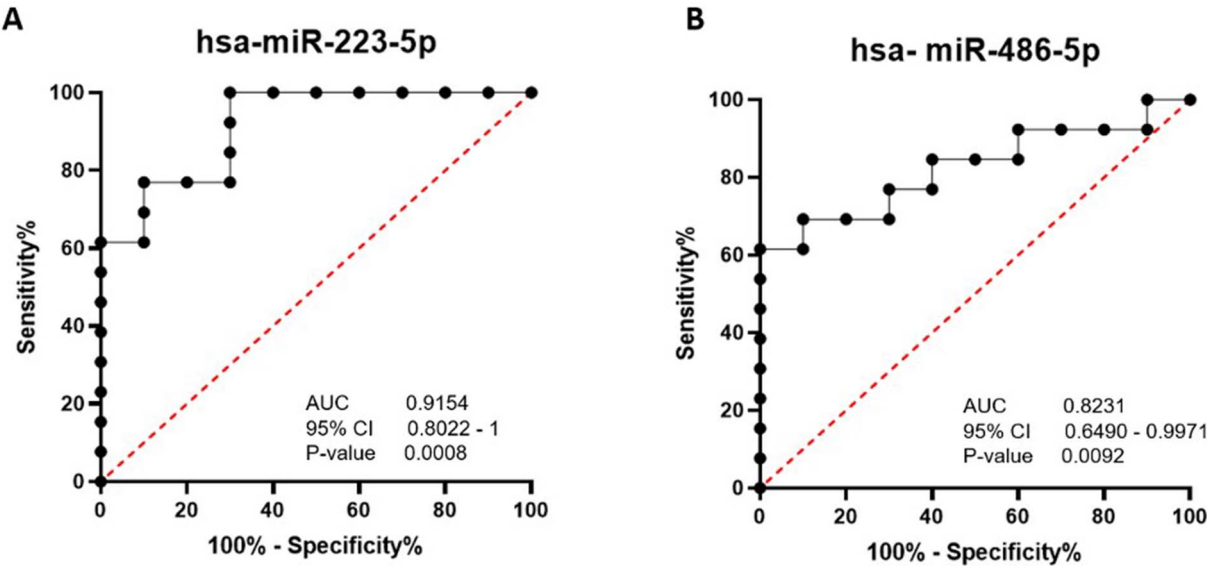


Figure 4. Area under the ROC curve for miRNAs based on the RT-qPCR data. (A) hsa-miRNA-223-5p, and (B) hsa-miRNA-486-5p.

(Llorens-Revull *et al.*, 2023). In a recent study that isolated EVs via UC, EV-derived miR-150-5p and miR-15b-5p were identified in patients infected with *P. vivax*. Furthermore, upregulation of let-7a-5p was observed in both *P. vivax* and *P. falciparum* infections (Ketprasit *et al.*, 2020). The miR-223 is involved in the proliferation and function of granulocytes and platelets (Fazi *et al.*, 2005; Shi *et al.*, 2015), implying that platelets and granulocytes might serve as potential sources of EVs during *P. knowlesi* infection. The upregulation of miR-223 in platelets is associated with increased platelet activation and aggregation (Gatsiou *et al.*, 2012). During malaria infection, iRBCs could interact with platelets, leading to the release of chemokines and inflammatory cytokines (Srivastava and Srivastava, 2015). Hsa-miR-223 also forms complexes with

lipoproteins circulating in the blood (Vickers *et al.*, 2011). LDL has been observed interacting with the surface of EVs, making it interesting to determine whether this interaction is the result of contamination from the circulation. Isolating EVs from lipoproteins in the blood is still challenging due to the overwhelming abundance of lipoproteins, exceeding EVs by at least 10⁵-fold (Zhang *et al.*, 2020). SEC is effective in largely eliminating high-density lipoprotein, although LDL of comparable density might be co-isolated with EVs. Employing subsequent UC as a washing step can aid in minimizing contamination (Koster *et al.*, 2021). miR-223 has been documented as being upregulated in sickle cell erythrocytes infected with *P. falciparum* (LaMonte *et al.*, 2012) and in the plasma of *P. vivax* patients (Hadighi *et al.*, 2022).

Moreover, in mice with cerebral malaria, miR-223-3p, miR-19b-3p and miR-142-3p exhibited significant upregulation compared to non-infected mice (Martin-Alonso et al., 2018).

Computational target predictions were conducted for hsa-miR-223-5p and hsa-miR-486-5p on both human and malaria transcripts, along with an enrichment analysis in GO and KEGG pathways. The prediction indicated that hsa-miR-223-5p targets several human transcripts including hepatocyte growth factor (HGF), MET proto-oncogene (MET), vascular cell adhesion molecule 1 (VCAM-1), toll-like receptor 4 (TLR4), myeloid differentiation primary response 88 (MyD88), glycophorin A (GYPA), glycophorin C (GYPC) and CD40 molecule (CD40). The HGF/MET signalling pathway plays a critical role in diverse cellular processes such as cell growth, survival, motility and morphogenesis (Organ and Tsao, 2011). Moreover, it is essential for the initial development of parasites within the host liver by preventing cell apoptosis and involving host-cell actin cytoskeleton reorganization (Carrolo et al., 2003). VCAM-1 contains 6 or 7 immunoglobulin domains, is expressed on endothelial cells in blood vessels, and acts as a cell adhesion molecule (Cook-Mills et al., 2011). The elevated VCAM-1 expression is associated with the sequestration of *P. falciparum* in vessels, particularly in severe cases (Armah et al., 2005). TLR4 is expressed in immune cells including monocytes, macrophages, B cells, dendritic cells and epithelial cells. Monocytes expressing TLR4 are activated by parasite-derived GPI anchors and hemozoin, leading to the production of pro-inflammatory cytokines. MyD88 acts as a key signalling protein, connecting the activated receptors with downstream signalling molecules. MyD88 activation leads to the activation of transcription factors such as NF- κ B and MAPKs, which results in the production of pro-inflammatory cytokines like IL-1, TNF- α and IL-6 (Dobbs et al., 2020). GYPA and GYPC are cell surface receptors found on red blood cells that engage with parasite antigens such as EBA-175 and EBA-140, facilitating the invasion of parasites (Jaskiewicz et al., 2019). In this study, all predicted human host targets of hsa-miR-223-5p were found to be associated with specific biological processes and CCs based on GO analysis. These targets are enriched in processes like phagocytosis, cellular response to mechanical stimuli, and NF- κ B activation, which are critical for immune cell function and host defence. The enriched CCs include the cell surface, integral components of the plasma membrane and the plasma membrane, emphasizing the role of miR-223-5p in membrane-related immune interactions. Based on these findings, we hypothesized that miR-223-5p may target HGF, which acts as an anti-inflammatory mediator. If miR-223-5p reduces HGF levels, immune responses could shift toward a more pro-inflammatory state, thereby activating pathways such as NF- κ B, TLR4 and MyD88 (Zhou et al., 2018). A previous study suggested a role for miRNAs in modulating inflammatory signalling pathways (Lee et al., 2021); however, direct evidence linking miR-223-5p to HGF suppression and subsequent activation of pro-inflammatory processes remains limited. Further experimental validation is needed to clarify whether miR-223-5p directly influences HGF-mediated immune modulation during *P. knowlesi* infection. Additionally, while miR-223-5p overexpression may help regulate inflammation and prevent tissue damage, it could also compromise the immune system's ability to clear the *Plasmodium* parasite, which utilizes various immune evasion strategies (Su et al., 2025). Moreover, it is important to note that hsa-miR-223-5p can exert varying effects on its target genes, depending on factors such as its subcellular location, expression level, the degree of complementarity with the target and other regulatory elements in the cellular environment (O'Brien et al., 2018). Further

investigation is needed to clarify its specific role in *P. knowlesi* infection.

Our results indicated an increase in hsa-miR-486-5p expression in plasma-derived EVs from *P. knowlesi*-infected patients. This finding concurred with a previous study, wherein miRNA profiling of EVs isolated from *P. falciparum* culture revealed that hsa-miR-486-5p exhibited one of the highest expression levels (Babatunde et al., 2018). MiR-486-5p is expressed abundantly in RBCs and is involved in RBC maturation. CD40 was predicted as the target of miR-486-5p. CD40, a membrane glycoprotein, is prominently expressed in B lymphocytes, dendritic cells, monocytes and platelets. CD40 expression is induced by pro-inflammatory factors and regulated by transcriptional factors including NF- κ B, responsible for the inflammatory response (Antoniades et al., 2009). The results of this study demonstrated that miR-486-5p was enriched in protein binding and cytosol. Moreover, the parasite mRNA has been predicted as a target of human miR-223-5p, with the *SICAvar* gene being the most frequently identified target in the database. The *P. knowlesi* schizont-infected cell agglutination (SICA) var gene family, expressed on the surface of infected erythrocytes, codes for antigenic variation, analogous to the virulence-associated *PfEMP1* gene (Lapp et al., 2013). The *SICAvar* gene is associated with cytoadhesion of *P. knowlesi* iRBCs with endothelial cells in the umbilical vein and the gastrointestinal tract (Chuang et al., 2022; Peterson et al., 2022). EVs are found to harbour promising miRNA candidates, serving as robust biomarkers with an AUC close to 1. This characteristic makes them valuable for diagnostic purposes. The resistance of miRNAs to degradation, facilitated by their protection within vesicles during circulation, adds to the appeal of exosome miRNAs as stable and reliable disease biomarkers. However, the sorting process of miRNAs in EVs is not well understood and may exhibit either selective or non-selective characteristics, potentially influenced by the subtypes of EVs (Temoche-Diaz et al., 2019). Recognition by RNA-binding proteins such as hnRNP A2B1 and Argonaute-2, specific structural features, post-transcriptional modifications of miRNA and cellular content can contribute to the loading of miRNAs into EVs (Qiu et al., 2021). Our findings shed light on miRNAs associated with *P. knowlesi* infection, providing valuable insights into their molecular mechanisms. Further research is required to explore the role of miRNAs in malaria pathogenesis. In-depth *in vitro* and *in vivo* studies, along with investigations in human populations are required to confirm these findings and assess the potential of miRNAs as a therapeutic target or diagnostic marker.

Conclusions

This study established a foundation for understanding the pathophysiology of *P. knowlesi*, highlighting the increased expression of EV-miRNAs, specifically hsa-miR-223-5p and hsa-miR-486-5p, which could reflect the underlying processes of *P. knowlesi* infection. Further studies should validate the functionality of EV-miRNAs, as they have the potential to provide crucial insights to develop new diagnostic or patient monitoring biomarkers.

Author contributions. Conceptualization: ST and RN, Software: TK and NN, Investigation: TK and PM. Resources: CW, JS, SJ, CR, and RN, Formal Analysis: HB, KS, NT, RP, CS, and NS, Writing – Original Draft Preparation: TK and ST, Writing – Revised Draft and Editing: ST, RN, HB, JS, and CW. All authors have read and approved the final version of the revised manuscript. RN and ST contributed equally as co-corresponding authors.

Financial support. This research was supported by Prince of Songkla University (Grant No. MET6602031S and MET6402038S), National Science, Research and Innovation Fund (NSRF) and Prince of Songkla University (Grant No. MET6601206S), PSU Ph.D. Scholarship contract No. PSU_PHD2562-004, the NSRF via the Program Management Unit for Human Resources & Institutional Development, Research and Innovation (Grant No. B13F660074) and Thailand Science Research and Innovation (TSRI), Chulabhorn Research Institute (grant number 49890/4759798).

Competing interests. The authors declare no competing interests.

Ethical standards. All samples were obtained as leftover specimens from routine laboratory procedures. This study received ethical approval from the Ethics Committee of the Faculty of Medical Technology, Prince of Songkla University, under approval number EC66-03.

References

- Abels ER and Breakefield XO (2016) Introduction to extracellular vesicles: Biogenesis, RNA cargo selection, content, release, and uptake. *Cellular and Molecular Neurobiology* 36(3), 301–312. doi:10.1007/s10571-016-0366-z
- Anstey NM, Grigg MJ, Rajahram GS, Cooper DJ, William T, Kho S and Barber BE (2021) Knowlesi malaria: Human risk factors, clinical spectrum, and pathophysiology. *Advances in Parasitology* 113, 1–43. doi:10.1016/bs.apar.2021.08.001
- Antoniades C, Bakogiannis C, Tousoulis D, Antonopoulos AS and Stefanadis C (2009) The CD40/CD40 ligand system: Linking inflammation with atherothrombosis. *Journal of the American College of Cardiology* 54(8), 669–677. doi:10.1016/j.jacc.2009.03.076
- Armah H, Wired EK, Dodoo AK, Adjei AA, Tettey Y and Gyasi R (2005) Cytokines and adhesion molecules expression in the brain in human cerebral malaria. *International Journal of Environmental Research & Public Health* 2(1), 123–131. doi:10.3390/ijerph2005010123
- Avalos-Padilla Y, Georgiev VN, Lantero E, Pujals S, Verhoef R, N Borgheti-Cardoso L, Albertazzi L, Dimova R and Fernández-Busquets X (2021) The ESCRT-III machinery participates in the production of extracellular vesicles and protein export during *Plasmodium falciparum* infection. *PLOS Pathogens* 17(4), e1009455. doi:10.1371/journal.ppat.1009455
- Babatunde KA, Mbagwu S, Hernández-Castañeda MA, Adapa SR, Walch M, Filgueira L, Falquet L, Jiang RHY, Ghiran I and Mantel PY (2018) Malaria infected red blood cells release small regulatory RNAs through extracellular vesicles. *Scientific Reports* 8(1), 884. doi:10.1038/s41598-018-19149-9
- Babatunde KA, Yesodha Subramanian B, Ahouidi AD, Martinez Murillo P, Walch M and Mantel PY (2020) Role of extracellular vesicles in cellular cross talk in malaria. *Frontiers in Immunology* 11, 22. doi:10.3389/fimmu.2020.00022
- Canatan D, Yilmaz O, Sonmez Y, Cim A, Baykara M, Savas M, Coskun HS, Goksu SS and Aktekin MR (2022) Use of MicroRNAs as biomarkers in the early diagnosis of prostate cancer. *Acta Bio-medica: Atenei Parmensis* 93(3), e2022089. doi:10.23750/abm.v93i3.11642
- Carrolo M, Giordano S, Cabrita-Santos L, Corso S, Vigário AM, Silva S, Leirião P, Carapau D, Armas-Portela R, Comoglio PM, Rodriguez A and Mota MM (2003) Hepatocyte growth factor and its receptor are required for malaria infection. *Nature Medicine* 9(11), 1363–1369. doi:10.1038/nm947
- Chakrabarti M, Garg S, Rajagopal A, Pati S and Singh S (2020) Targeted repression of *Plasmodium apicortin* by host microRNA impairs malaria parasite growth and invasion. *Disease Models and Mechanisms* 13(6), dmm042820. doi:10.1242/dmm.042820
- Chamnanchanunt S, Kuroki C, Desakorn V, Enomoto M, Thanachartwet V, Sahassananda D, Sattabongkot J, Jenwithisuk R, Fucharoen S, Svasti S and Umemura T (2015) Downregulation of plasma miR-451 and miR-16 in *Plasmodium vivax* infection. *Experimental Parasitology* 155, 19–25. doi:10.1016/j.exppara.2015.04.013
- Chantaramongkol J and Buathong R (2016) A fatal malaria caused by *Plasmodium knowlesi* infection in a healthy man, Betong, Yala, Thailand April, 2016. *International Journal of Infectious Diseases* 53, 124.
- Chuang H, Sakaguchi M, Lucky AB, Yamagishi J, Katakai Y, Kawai S and Kaneko O (2022) SICA-mediated cytoadhesion of *Plasmodium knowlesi*-infected red blood cells to human umbilical vein endothelial cells. *Scientific Reports* 12(1), 14942. doi:10.1038/s41598-022-19199-0
- Combes V, Taylor TE, Juhan-Vague I, Mège JL, Mwenenchanya J, Tembo M, Grau GE and Molyneux ME (2004) Circulating endothelial microparticles in malawian children with severe falciparum malaria complicated with coma. *Journal of the American Medical Association* 291(21), 2542–2544. doi:10.1001/jama.291.21.2542-b
- Cook-Mills JM, Marchese ME and Abdala-Valencia H (2011) Vascular cell adhesion molecule-1 expression and signaling during disease: Regulation by reactive oxygen species and antioxidants. *Antioxidants & Redox Signaling* 15(6), 1607–1638. doi:10.1089/ars.2010.3522
- Cox-Singh J, Hiu J, Lucas SB, Divis PC, Zulkarnaen M, Chandran P, Wong KT, Adem P, Zaki SR, Singh B and Krishna S (2010) Severe malaria - a case of fatal *Plasmodium knowlesi* infection with post-mortem findings: A case report. *Malaria Journal* 9, 10. doi:10.1186/1475-2875-9-10.
- Dai X, Zhuang Z and Zhao PX (2018) psRNATarget: a plant small RNA target analysis server (2017 release). *Nucleic acids research* 46(W1), W49–W54. doi:10.1093/nar/gky316
- Dandewad V, Bindu A, Joseph J and Seshadri V (2019) Import of human miRNA-RISC complex into *Plasmodium falciparum* and regulation of the parasite gene expression. *Journal of Biosciences* 44(2), 50.
- Dobbs KR, Crabtree JN and Dent AE (2020) Innate immunity to malaria-The role of monocytes. *Immunological Reviews* 293(1), 8–24. doi:10.1111/imr.12830
- Fazi F, Rosa A, Fatica A, Gelmetti V, De Marchis ML, Nervi C and Bozzoni I (2005) A microcircuitry comprised of microRNA-223 and transcription factors NF1-A and C/EBPα regulates human granulopoiesis. *Cell* 123(5), 819–831. doi:10.1016/j.cell.2005.09.023
- Gatsiou A, Boeckel JN, Randriamboavonjy V and Stellos K (2012) MicroRNAs in platelet biogenesis and function: Implications in vascular homeostasis and inflammation. *Current Vascular Pharmacology* 10(5), 524–531. doi:10.2174/157016112801784611
- Gupta H, Rubio M, Siteo A, Varo R, Cisteró P, Madrid L, Cuamba I, Jimenez A, Martiáñez-Vendrell X, Barrios D, Pantano L, Brimacombe A, Bustamante M, Bassat Q and Mayor A (2021) Plasma microRNA profiling of *Plasmodium falciparum* biomass and association with severity of malaria disease. *Emerging Infectious Diseases* 27(2), 430–442. doi:10.3201/eid2702.191795
- Hadighi R, Heidari A, Fallah P, Keshavarz H, Tavakoli Z, Mansouri S and Sadrkhanloo M (2022) Key plasma microRNAs variations in patients with *Plasmodium vivax* malaria in Iran. *Heliyon* 8(3), e09018. doi:10.1016/j.heliyon.2022.e09018
- Jaskiewicz E, Jodłowska M, Kaczmarek R and Zerka A (2019) Erythrocyte glycoporphins as receptors for *Plasmodium* merozoites. *Parasites and Vectors* 12(1), 317. doi:10.1186/s13071-019-3575-8
- Ketprasit N, Cheng IS, Deutsch F, Tran N, Imwong M, Combes V and Palasuwan D (2020) The characterization of extracellular vesicles-derived microRNAs in Thai malaria patients. *Malaria Journal* 19(1), 285. doi:10.1186/s12936-020-03360-z
- Koster HJ, Rojalin T, Powell A, Pham D, Mizenko RR, Birkeland AC and Carney RP (2021) Surface enhanced Raman scattering of extracellular vesicles for cancer diagnostics despite isolation dependent lipoprotein contamination. *Nanoscale* 13(35), 14760–14776. doi:10.1039/d1nr03334d
- LaMonte G, Philip N, Reardon J, Lacsina JR, Majoros W, Chapman L, Thornburg CD, Telen MJ, Ohler U, Nicchitta CV, Haystead T and Chi JT (2012) Translocation of sickle cell erythrocyte microRNAs into *Plasmodium falciparum* inhibits parasite translation and contributes to malaria resistance. *Cell Host & Microbe* 12(2), 187–199. doi:10.1016/j.chom.2012.06.007
- Lapp SA, Korir-Morrison C, Jiang J, Bai Y, Corredor V and Galinski MR (2013) Spleen-dependent regulation of antigenic variation in malaria parasites: *Plasmodium knowlesi* SICAvar expression profiles in splenic and asplenic hosts. *PLoS One* 8(10), e78014. doi:10.1371/journal.pone.0078014
- Lee L, Howitt B, Cheng T, King M, Stawiski K, Fendler W, Chowdhury D, Matulonis U and Konstantinopoulos PA (2021) MicroRNA profiling in a case-control study of African American women with uterine serous carcinoma. *Gynecologic Oncology* 163(3), 453–458.

- Llorens-Revull M, Martínez-González B, Quer J, Esteban JI, Núñez-Moreno G, Mínguez P, Burgui I, Ramos-Ruiz R, Soria ME, Rico A, Riveiro-Barciela M, Saulea S, Piron M, Corrales I, Borràs FE, Rodríguez-Frías F, Rando A, Ramírez-Serra C, Camós S, Domingo E and Costafreda MI (2023) Comparison of extracellular vesicle isolation methods for miRNA sequencing. *International Journal of Molecular Sciences* **24**(15), 12183. doi:10.3390/ijms241512183
- Lodde V, Floris M, Muroi MR, Cucca F and Idda ML (2022) Non-coding RNAs in malaria infection. *Wiley Interdisciplinary Reviews RNA* **13**(3), e1697. doi:10.1002/wrna.1697
- Mantel PY, Hjelmqvist D, Walch M, Kharoubi-Hess S, Nilsson S, Ravel D, Ribeiro M, Grüning C, Ma S, Padmanabhan P, Trachtenberg A, Ankarleev J, Brancucci NM, Huttenhower C, Duraisingh MT, Ghiran I, Kuo WP, Filgueira L, Martinelli R and Marti M (2016) Infected erythrocyte-derived extracellular vesicles alter vascular function via regulatory Ago2-miRNA complexes in malaria. *Nature Communications* **7**, 12727. doi:10.1038/ncomms12727
- Mantel PY, Hoang AN, Goldowitz I, Potashnikova D, Hamza B, Vorobjev I, Ghiran I, Toner M, Irimia D, Ivanov AR, Barteneva N and Marti M (2013) Malaria-infected erythrocyte-derived microvesicles mediate cellular communication within the parasite population and with the host immune system. *Cell Host & Microbe* **13**(5), 521–534. doi:10.1016/j.chom.2013.04.009
- Martin-Alonso A, Cohen A, Quispe-Ricalde MA, Foronda P, Benito A, Berzosa P, Valladares B and Grau GE (2018) Differentially expressed microRNAs in experimental cerebral malaria and their involvement in endocytosis, adherens junctions, FoxO and TGF- β signalling pathways. *Scientific Reports* **8**(1), 11277. doi:10.1038/s41598-018-29721-y
- Minwuyet A and Abiye M (2022) Role of secretory vesicles derived from *Plasmodium* infected red blood cells to the pathogenesis of malaria: A review. *Advanced Techniques in Biology & Medicine* **10**, 360.
- O'Brien J, Hayder H, Zayed Y and Peng C (2018) Overview of MicroRNA Biogenesis, Mechanisms of Actions, and Circulation. *Front Endocrinol (Lausanne)* **9**, 402. doi:10.3389/fendo.2018.00402
- Opadokun T and Rohrbach P (2021) Extracellular vesicles in malaria: An agglomeration of two decades of research. *Malaria Journal* **20**(1), 442. doi:10.1186/s12936-021-03969-8
- Organ SL and Tsao MS (2011) An overview of the c-MET signaling pathway. *Therapeutic Advances in Medical Oncology* **3**(1 Suppl), S7–S19. doi:10.1177/1758834011422556
- Pankoui Mfonkeu JB, Gouado I, Fotso Kuaté H, Zambou O, Amvam Zollo PH, Grau GE and Combes V (2010) Elevated cell-specific microparticles are a biological marker for cerebral dysfunctions in human severe malaria. *PLoS One* **5**(10), e13415. doi:10.1371/journal.pone.0013415
- Peterson MS, Joyner CJ, Lapp SA, Brady JA, Wood JS, Cabrera-Mora M, Saney CL, Fonseca LL, Cheng WT, Jiang J, Soderberg SR, Nural MV, Hankus A, Machiah D, Karpuzoglu E, DeBarry JD, Tirouvanziam R, Kissinger JC, Moreno A, Gumber S and Galinski MR (2022) *Plasmodium knowlesi* cytoadhesion involves SICA variant proteins. *Frontiers in Cellular and Infection Microbiology* **12**, 888496. doi:10.3389/fcimb.2022.888496
- Putaporntip C, Buppan P and Jongwutiwes S (2011) Improved performance with saliva and urine as alternative DNA sources for malaria diagnosis by mitochondrial DNA-based PCR assays. *Clinical Microbiology and Infection* **17**(10), 1484–1491. doi:10.1111/j.1469-0691.2011.03507.x
- Qiu Y, Li P, Zhang Z and Wu M (2021) Insights into exosomal non-coding RNAs sorting mechanism and clinical application. *Frontiers in Oncology* **11**, 664904. doi:10.3389/fonc.2021.664904
- Rajahram GS, Barber BE, William T, Menon J, Anstey NM and Yeo TW (2012) Deaths due to *Plasmodium knowlesi* malaria in Sabah, Malaysia: Association with reporting as *Plasmodium malariae* and delayed parenteral artesunate. *Malaria Journal* **11**, 284. doi:10.1186/1475-2875-11-284
- Rangel G, Teerawattapanong N, Chamnanchanunt S, Umemura T, Pinyachat A and Wanram S (2019) Candidate microRNAs as biomarkers in malaria infection: A systematic review. *Current Molecular Medicine* **20**(1), 36–43. doi:10.2174/1566524019666190820124827
- Rathjen T, Nicol C, McConkey G and Dalmay T (2006) Analysis of short RNAs in the malaria parasite and its red blood cell host. *FEBS Letters* **580**(22), 5185–5188. doi:10.1016/j.febslet.2006.08.063
- Regev-Rudzki N, Wilson DW, Carvalho TG, Sisquella X, Coleman BM, Rug M, Bursac D, Angrisano F, Gee M, Hill AF, Baum J and Cowman AF (2013) Cell-cell communication between malaria-infected red blood cells via exosome-like vesicles. *Cell* **153**(5), 1120–1133. doi:10.1016/j.cell.2013.04.029
- Sahu U, Sahoo PK, Kar SK, Mohapatra BN and Ranjit M (2013) Association of TNF level with production of circulating cellular microparticles during clinical manifestation of human cerebral malaria. *Human Immunology* **74**(6), 713–721. doi:10.1016/j.humimm.2013.02.006
- Santos MLS, Coimbra RS, Sousa TN, Guimarães LFF, Gomes MS, Amaral LR, Pereira DB, Fontes CJF, Hawwari I, Franklin BS and Carvalho LH (2021) The interface between inflammatory mediators and microRNAs in *Plasmodium vivax* severe Thrombocytopenia. *Frontiers in Cellular & Infection Microbiology* **11**, 631333. doi:10.3389/fcimb.2021.631333
- Schuster SL and Hsieh AC (2019) The Untranslated Regions of mRNAs in Cancer. *Trends Cancer* **5**(4), 245–262. doi:10.1016/j.trecan.2019.02.011
- Shi R, Zhou X, Ji WJ, Zhang YY, Ma YQ, Zhang JQ and Li YM (2015) The emerging role of miR-223 in platelet reactivity: Implications in antiplatelet therapy. *BioMed Research International* **2015**, 981841. doi:10.1155/2015/981841
- Sisquella X, Ofir-Birin Y, Pimentel MA, Cheng L, Abou Karam P, Sampaio NG, Penington JS, Connolly D, Giladi T, Scicluna BJ, Sharples RA, Waltmann A, Avni D, Schwartz E, Schofield L, Porat Z, Hansen DS, Papenfuss AT, Eriksson EM, Gerlic M, Hill AF, Bowie AG and Regev-Rudzki N (2017) Malaria parasite DNA-harboring vesicles activate cytosolic immune sensors. *Nature communications* **8**(1), 1985. doi:10.1038/s41467-017-02083-1
- Srivastava K and Srivastava K (2015) Role of platelet-mediated cytoadherence and chemokines release in severe malaria. *SOJ Immunology* **3**(3), 1–6. doi:10.15226/soji/3/3/00132
- Su XZ, Xu F, Stadler RV, Teklemichael AA and Wu J (2025) Malaria: Factors affecting disease severity, immune evasion mechanisms, and reversal of immune inhibition to enhance vaccine efficacy. *PLOS Pathogens* **21**(1), e1012853.
- Temoche-Diaz MM, Shurtleff MJ, Nottingham RM, Yao J, Fadadu RP, Lambowitz AM and Schekman R (2019) Distinct mechanisms of microRNA sorting into cancer cell-derived extracellular vesicle subtypes. *eLife* **8**, e47544. doi:10.7554/eLife.47544
- ThaiMoPH (2024) Thailand Malaria Elimination Program. Ministry of Public Health, Thailand. Available at https://malaria.ddc.moph.go.th/malariaR10/index_newversion.php (accessed 31 November 2024).
- Théry C, Witwer KW, Aikawa E, Alcaraz MJ, Anderson JD, Andriantsitohaina R, Antoniou A, Arab T, Archer F, Atkin-Smith GK, Ayre DC, Bach JM, Bachurski D, Baharvand H, Balaj L, Baldacchino S, Bauer NN, Baxter AA, Bebawy M, Beckham C and Zuba-Surma EK (2018) Minimal information for studies of extracellular vesicles 2018 (MISEV2018): A position statement of the International Society for Extracellular Vesicles and update of the MISEV2014 guidelines. *Journal of Extracellular Vesicles* **7**(1), 1535750. doi:10.1080/20013078.2018.1535750
- Toda H, Diaz-Varela M, Segui-Barber J, Roobsoong W, Baro B, Garcia-Silva S, Galiano A, Gualdrón-López M, Almeida ACG, Brito MAM, de Melo GC, Aparici-Herraiz I, Castro-Cavada C, Monteiro WM, Borràs E, Sabido E, Almeida IC, Chojnacki J, Martínez-Picado J, Calvo M and Del Portillo HA (2020) Plasma-derived extracellular vesicles from *Plasmodium vivax* patients signal spleen fibroblasts via NF- κ B facilitating parasite cytoadherence. *Nature Communications* **11**(1), 2761. doi:10.1038/s41467-020-16337-y
- Vickers KC, Palmisano BT, Shoucri BM, Shamburek RD and Remaley AT (2011) MicroRNAs are transported in plasma and delivered to recipient cells by high-density lipoproteins. *Nature Cell Biology* **13**(4), 423–433. doi:10.1038/ncb2210
- Wang Z, Xi J, Hao X, Deng W, Liu J, Wei C, Gao Y, Zhang L and Wang H (2017) Red blood cells release microparticles containing human argonaute 2 and miRNAs to target genes of *Plasmodium falciparum*. *Emerging Microbes & Infections* **6**(8), e75. doi:10.1038/emi.2017.63

- Xu D, Di K, Fan B, Wu J, Gu X, Sun Y, Khan A, Li P and Li Z** (2022) MicroRNAs in extracellular vesicles: Sorting mechanisms, diagnostic value, isolation, and detection technology. *Frontiers in Bioengineering and Biotechnology* **10**, 948959. doi:[10.3389/fbioe.2022.948959](https://doi.org/10.3389/fbioe.2022.948959).
- Xue X, Zhang Q, Huang Y, Feng L and Pan W** (2008) No miRNA were found in *Plasmodium* and the ones identified in erythrocytes could not be correlated with infection. *Malaria Journal* **7**, 47. doi:[10.1186/1475-2875-7-47](https://doi.org/10.1186/1475-2875-7-47).
- Zhang X, Borg EGF, Liaci AM, Vos HR and Stoorvogel W** (2020) A novel three step protocol to isolate extracellular vesicles from plasma or cell culture medium with both high yield and purity. *Journal of Extracellular Vesicles* **9**(1), 1791450. doi:[10.1080/20013078.2020.1791450](https://doi.org/10.1080/20013078.2020.1791450)
- Zhou W, Pal AS, Hsu AY, Gurol T, Zhu X, Wirbisky-Hershberger SE, Freeman JL, Kasinski AL and Deng Q** (2018) MicroRNA-223 suppresses the canonical NF- κ B pathway in basal keratinocytes to Dampen neutrophilic inflammation. *Cell Reports* **22**(7), 1810–1823.